

DETERMINATION OF FIELDS NEAR AN ICRH ANTENNA USING A 3D MAGNETOSTATIC LAPLACE FORMULATION*

P.M. Ryan, K.E. Rothe, J.H. Whealton, and D.W. Swain
Oak Ridge National Laboratory, Oak Ridge, TN 37831

ABSTRACT

In the vicinity of an ICRH antenna strap, where there are no volume currents and a free-space wavelength is much longer than the dimensions of interest, Ampere's law reduces to a curl-free condition on the magnetic field, allowing a magnetic scalar potential to be defined. This scalar potential is a solution of the three-dimensional (3D) Laplace equation and satisfies the following boundary conditions on the magnetic field: (1) the line integral of the magnetic field around the current strap is equal to the current flowing in the strap and (2) the perpendicular component of the magnetic field vanishes at conductor surfaces (no flux penetration of perfect conductors). This formulation allows for the magnetic field solution of quite complex 3D geometries, such as poloidal current straps with asymmetric radial feeds or detailed Faraday shield geometries.

INTRODUCTION

The design, evaluation, and optimization of ICRH antennas requires knowledge of the electromagnetic fields generated by the 3D launcher structure. Such knowledge permits evaluation of the antenna coupling and power density distribution, as well as the power transmission, reflection, and absorption of the Faraday shield. A 3D magnetostatic analysis has been developed to meet the following requirements:

- (1) the ability to specify and modify the geometry of the structure quickly and easily, thus facilitating optimization studies;
- (2) the reduction of computation time needed for a given degree of accuracy;
- (3) the ability to treat a localized area of a large structure, such as the region of a Faraday shield element, in greater detail;
- (4) the self-consistent calculation of current distributions, within the constraints of the model.

THE MAGNETOSTATIC MODEL

The analysis uses Ampere's law, Fourier-analyzed in time and space:

$$\nabla \times \mathbf{B} = -j \mathbf{k} \times \mathbf{B} = \mu_0 \mathbf{J} + j\omega \mu_0 \epsilon_0 \mathbf{E} = j(k_0/c) \mathbf{E}, \quad (1)$$

where the current density \mathbf{J} vanishes in the solution domain. The long-wavelength approximation may be used when $k_0/k \approx L/\lambda \ll 1$, where L is the characteristic scale length of the device. This approximation decouples the electric and magnetic fields and reduces Ampere's law to the curl-free static representation

$$\nabla \times \mathbf{B} = 0. \quad (2)$$

This allows \mathbf{B} to be defined as the gradient of a scalar potential Ψ_m , which is a solution of Laplace's equation:

*Research sponsored by the Office of Fusion Energy, U.S. Department of Energy, under contract DE-AC05-84OR21400 with Martin Marietta Energy Systems, Inc.

$$\nabla \cdot \mathbf{B} = \nabla \cdot (\nabla \Psi_m) = \nabla^2 \Psi_m = 0. \quad (3)$$

Neumann boundary conditions are imposed on Ψ_m on all conducting surfaces, which ensures that the normal component of \mathbf{B} vanishes. The integral form of Ampere's law, which equates the total current flowing in the strap with the line integral of \mathbf{B} along any contour that encloses the strap, is used to set the Dirichlet boundary conditions on the remaining surfaces:

$$\oint_c \mathbf{B} \cdot d\mathbf{l} = 2 \int_{c_2} \nabla \Psi_m \cdot d\mathbf{l} = 2(\Psi_{m2} - \Psi_{m1}) = \mu_0 I, \quad (4)$$

where $\Psi_{m1} \equiv 0$ and $\Psi_{m2} \equiv \mu_0 I/2$.

APPLICATIONS

Figure 1 shows the geometry of a representative current strap in a recessed cavity; a radial current feed is attached to the top of the strap, and the bottom of the strap is grounded to the cavity. Figure 2 shows a similar geometry, except that the strap has been divided in the poloidal direction into two loops which are isolated from one another by a ground plane. This is done to reduce the maximum voltage that appears along the strap and to minimize the current falloff by decreasing the ratio of strap length to wavelength. The long-wavelength approximation used in these calculations implies constant current along the length of the strap, which is a design ideal. Typical ICRH loop antennas are designed to have $k_0/k \approx L/\lambda < 0.1$; these calculations may be modified by $\cos(\beta y)$ effects for electrically long antennas.

Figures 3(a) and 3(b) show the radial and toroidal components of the magnetic field near the first wall of the tokamak for the geometry of Fig. 1; the asymmetry in the fields is due to the asymmetry in the current feed. Figures 4(a) and 4(b) show the same field components for the poloidally stacked array of Fig. 2; the ground plane has introduced higher poloidal wave numbers into the spectrum. The relative power handling of these two antennas may be estimated by integrating the square of the magnetic field. For the current-limited case, in which all straps carry the same maximum current, the power is reduced by 25% for the poloidally stacked array; the poloidal extent of the strap is reduced by 14%; the total length of each strap, and hence the maximum voltage, is reduced by 36%. For the more typical voltage-limited case, keeping the maximum voltage constant allows the loop current to be increased by 56% and the total power to be increased by 83%. The actual power handling increase for this example may be higher, depending on the frequency of operation, owing to the neglected finite-wavelength effects.

This analysis will also be used to study the transmission properties of Faraday shield geometries. The magnetostatic approach allows one to consider only one poloidal period of the structure, as shown in Fig. 5 for a two-tier shield. The upper and lower boundaries are now symmetry planes and Neumann boundary conditions are imposed; the scale parameter for the long-wavelength approximation, L/λ , is typically around 10^{-3} in such geometries. The transmission and shielding properties of the shield will be found from comparison with the fields in the absence of the shield. The magnetic field at the shield surface is equated with the surface current, which can be used to estimate the eddy current losses in good conductors.

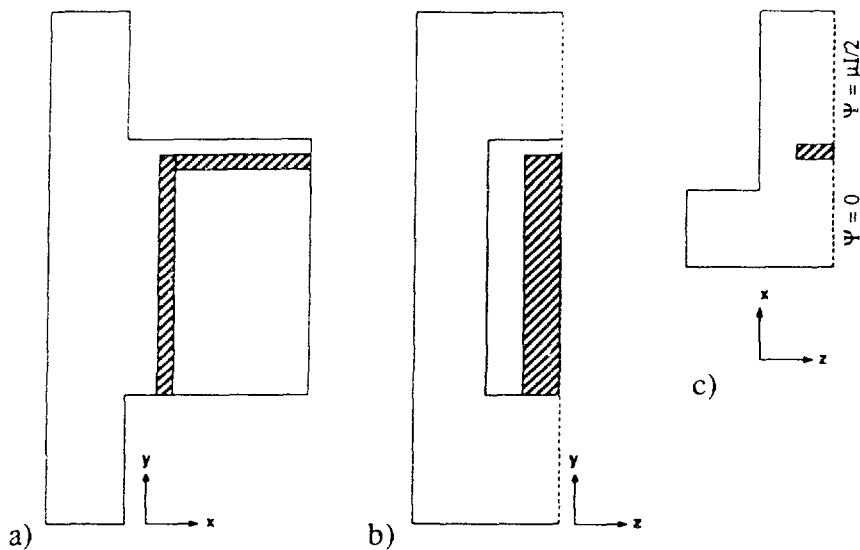


Fig. 1. Representative geometry for an asymmetrically fed current strap in a recessed cavity; (a) side view, (b) front view, (c) top view showing Dirichlet boundaries.

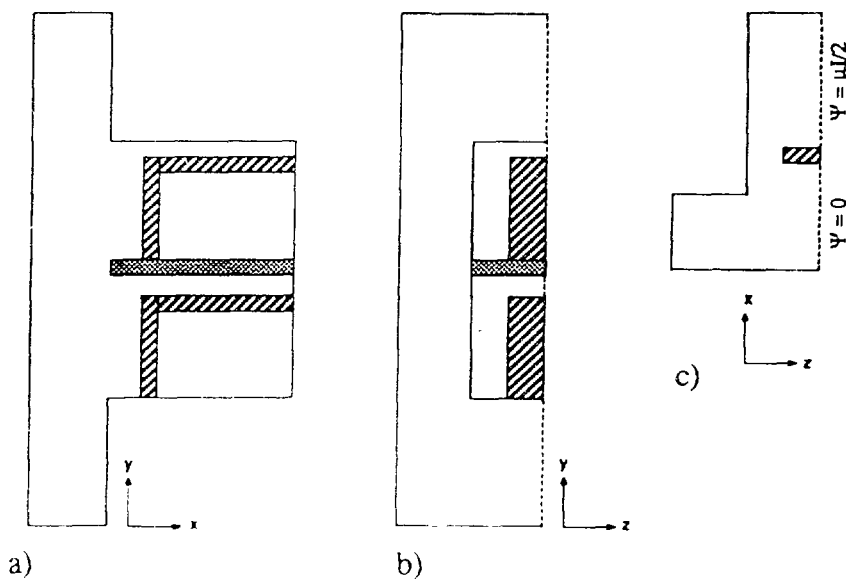


Fig. 2. Representative geometry for a poloidally stacked, isolated array.

This report was prepared as an account of work sponsored by an agency of the United States Government. Neither the United States Government nor any agency thereof, nor any of their employees, makes any warranty, express or implied, or assumes any legal liability or responsibility for the accuracy, completeness, or usefulness of any information, apparatus, product, or process disclosed, or represents that its use would not infringe privately owned rights. Reference herein to any specific commercial product, process, or service by trade name, trademark, manufacturer, or otherwise does not necessarily constitute or imply its endorsement, recommendation, or favoring by the United States Government or any agency thereof. The views and opinions of authors expressed herein do not necessarily state or reflect those of the United States Government or any agency thereof.

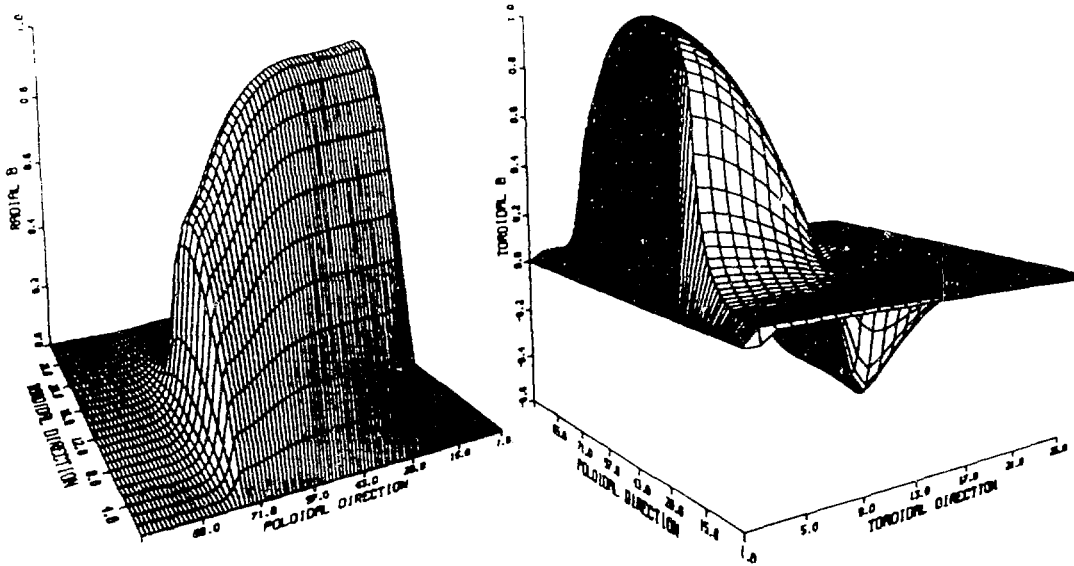


Fig. 3. (a) Radial and (b) toroidal magnetic field components close to the first wall for the antenna shown in Fig. 1.

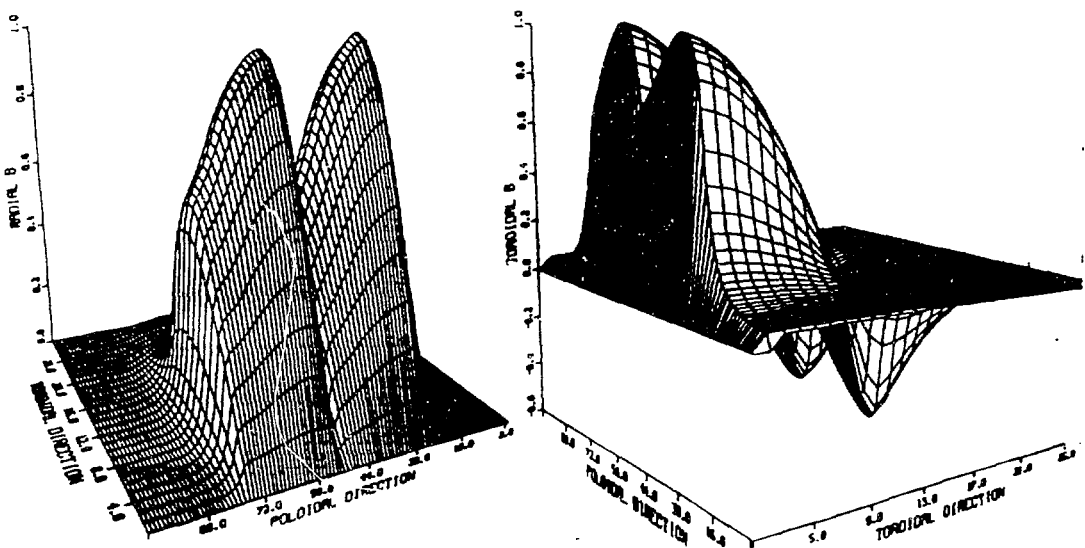


Fig. 4. (a) Radial and (b) toroidal magnetic field components close to the first wall for the antenna array shown in Fig. 2.

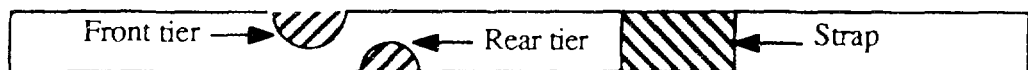


Fig. 5. Example of the poloidally periodic geometry used to model a two-tier Faraday shield (not drawn to scale)